THE JOURNAL OF PHYSICAL CHEMISTRY B LETTERS

2006, *110,* 11040−11043
Published on Web 05/17/2006

Metastability Release of the Form α of Trehalose by Isothermal Solid State Vitrification

J. F. Willart,* A. Hédoux, Y. Guinet, F. Danède, L. Paccou, F. Capet, and M. Descamps

Laboratoire de Dynamique et Structure des Matériaux Moléculaires, UMR CNRS 8024, ERT 1018 Université de Lille 1, Bât. P5, 59655 Villeneuve d'Ascq, France

Received: March 22, 2006; In Final Form: April 27, 2006

Kinetic investigations of the polymorphic form α of anhydrous trehalose have been performed below its apparent melting temperature (T_m) by differential scanning calorimetry (DSC) and X-ray diffraction. The results reveal a spontaneous isothermal vitrification process which indicates that the phase α is in a very unusual superheating situation. This behavior has been attributed to the fact that the effective melting temperature (T_m^{eff}) of the phase α is likely to be located far below the glass transition temperature (T_g) of this compound. The high viscosity of the liquid trehalose between T_m^{eff} and T_g is thus invoked to explain the long lifetime of the phase α in this temperature range.

1. Introduction

If the supercooling of a liquid is a common behavior, the superheating of a crystalline phase above its equilibrium melting temperature is, on the contrary, a much more unusual nonequilibrium situation that is difficult to reach. In the first case, the possibility to avoid the crystallization of a liquid upon cooling is greatly helped by the slowing down of the dynamics which increases the lifetime of the metastable liquid.[1,2] In the second case, the increase of the vibrational dynamics of the crystal upon heating has the opposite effect, making it increasingly difficult to superheat the crystalline phase above its melting temperature. Moreover, it is recognized that the melting process is easily triggered by a nearly unavoidable heterogeneous nucleation of the liquid at grain boundaries and free surfaces.[3−5] Despite these difficulties, some metallic systems have been successfully superheated by using sophisticated sample preparations able to reduce (or even suppress) the free surfaces of the samples (coating,[6] confinement,[7] clustering,[8] etc.) combined with powerful heating methods (internal heating,[9] ultrafast (10^{11} K/s) laser heating,[10] etc.). However, even under these conditions, the superheated crystals can generally only be obtained in narrow temperature ranges and exhibit relatively short lifetimes which makes them difficult to observe and to study.

Recently, it has been reported that the slow dehydration of trehalose dihydrate ($C_{12}H_{22}O_{11}\cdot 2H_2O$) produces a polymorphic phase (α) of anhydrous trehalose.[11−14] A most striking feature of this phase concerns its melting temperature (T_m = 123 °C) which is unusually located just above the glass transition temperature (T_g = 120 °C) of the corresponding liquid. Two interpretations have been put forward to explain this close-to-T_g melting.[14] The first one invokes a possible depression of the equilibrium melting temperature of the phase α which could result from a small crystallite size. This so-called Gibbs Thomson effect[15] could apply to the polymorphic phase α of trehalose whose small coherent spatial extent was strongly suggested by the structural analysis of its X-ray diffraction pattern.[14] In that case, the equilibrium melting temperature of the bulk crystalline phase would thus be at a much higher temperature. The second interpretation invokes, on the contrary, an effective melting temperature (T_m^{eff}) of the phase α which would be far below T_m. In that case, the phase α would be preserved between T_m^{eff} and T_g because the sub-T_g molecular mobility is too slow to drive readily the material toward the amorphous state. In that case, a rapid transformation can only occur just above T_g, leading to the apparent melting of the phase α at $T_m = T_g + 3$ °C in a typical experiment performed at 5 °C/min.

In this paper, we test the above second interpretation by investigating the stability of the phase α below T_g. The study has been performed through differential scanning calorimetry (DSC) and X-ray diffraction experiments after annealings of the phase α at different temperatures below T_g.

2. Experimental Section

α−α Trehalose Dihydrate (T_{2H_2O}). T_{2H_2O} was purchased from Fluka. It was more than 99% pure and was used without further purification.

Anhydrous Form α of Trehalose. The anhydrous form α of trehalose was obtained by annealing T_{2H_2O} at 50 °C under a dry nitrogen flow for 3 h. This was performed inside the DSC device using an open cell as explained in ref 14. It has been checked by thermogravimetric analysis that after this thermal treatment the sample is free of water.

Annealing Experiments. The annealing experiments of the phase α were performed inside the DSC device at 105, 110, and 117 °C for annealing times varying from 5 to 376 h. The visual inspection of the samples after these annealings has not revealed any sign of chemical degradation. Moreover, the physical properties (T_g, crystallization, melting, etc.) of the annealed samples have been found to be fully similar to those of a fresh pure compound. This also suggests the absence of chemical degradation.

Powder X-ray Diffraction (XRD) Experiments. The XRD experiments were performed with an Inel CPS 120 diffracto-

10.1021/jp061784r CCC: $33.50

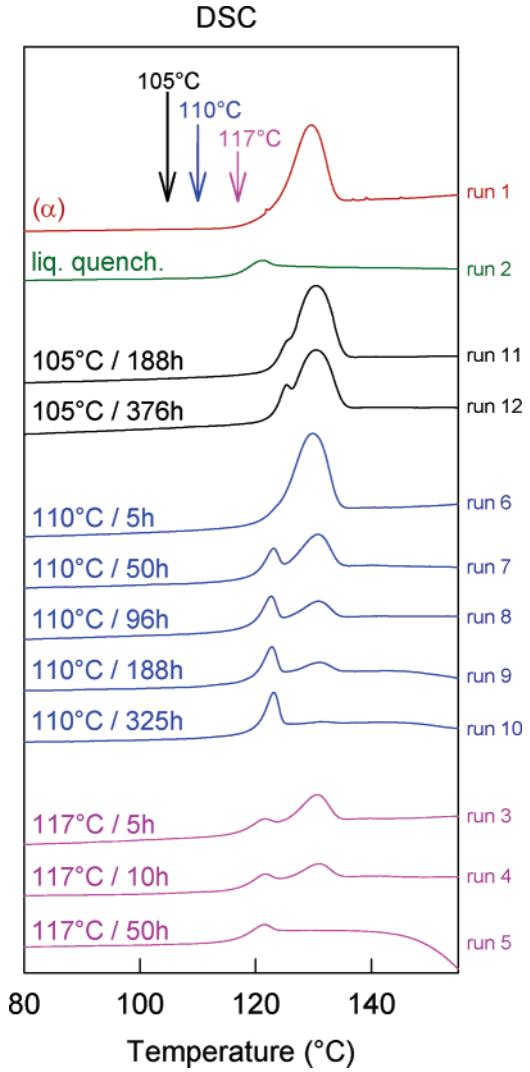

Figure 1. Thermograms obtained upon heating at 5 °C/min: (run 1) polymorphic form α of trehalose; (run 2) quenched liquid; (runs 3−12) polymorphic form α of trehalose after different annealing times below T_g. The annealing temperatures and the annealing times are reported on the left-hand side of the figure.

meter ($\lambda_{CuK\alpha 1} = 1.5405$ Å) equipped with a 120° curved position sensitive detector coupled to a 4096 channel analyzer. The samples were placed into Lindemann capillaries (∅ = 7 mm).

DSC Experiments. The DSC experiments were performed with the DSC 7 microcalorimeter of Perkin-Elmer. During all of the measurements, the calorimeter head was flushed with high purity nitrogen gas (water content <3 ppm). Temperature and enthalpy readings were calibrated using pure indium at the same scan rate (5 °C/min) as that used in the experiments.

3. Results

Figure 1 shows the DSC heating scan (5 °C/min) of trehalose after a variety of thermal treatments. Run 1 corresponds to the form α of trehalose. The thermogram shows a weak but well-defined melting peak (ΔH = 11.6 kJ/mol) at T_m = 123 °C. Run 2 corresponds to the quenched liquid trehalose. It shows a clear C_p jump which signals the glass transition at T_g = 120 °C. Runs 3−12 correspond to the phase α after different annealing times at 117, 110, and 105 °C, that is, below T_g and thus below $T_m = T_g + 3$. At 117 °C, increasing annealing times results in a decrease of the melting peak of the phase α in parallel with the development of a C_p jump characteristic of a glass transition (runs 3−5). After 50 h of annealing, the melting peak has totally disappeared while the C_p jump is found to be fully similar to that of the quenched liquid (run 2). This evolution reveals an isothermal vitrification process of the phase α below its melting temperature. At 110 °C, a similar but slower evolution is observed (runs 6−10). At this temperature, the full amorphization of the phase α is only reached after 325 h of annealing (run 10). At 105 °C, the amorphization process is still clearly detectable while too slow to be reasonably followed up to its completion. After 376 h of annealing (run 12), the amorphization fraction estimated from the melting enthalpy decrease is close to 10% and the C_p jump signaling the vitrification only appears through a shouldering on the left-hand wing of the melting peak. It must be noted that the endotherm which ends the C_p jump appears more and more developed as the annealing temperature is decreased. This feature simply reflects the recovery of the enthalpy lost during the annealing which is generally attributed to the relaxation of the structural short range order of the frozen amorphous material toward its metastable equilibrium state. The enthalpy recovery at T_g is thus expected to be all the larger, as the annealing has been performed at low temperature.

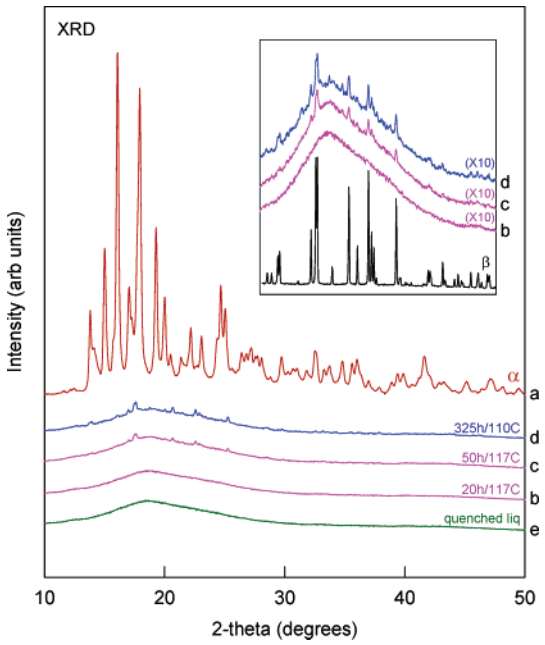

Figure 2. X-ray diffraction patterns recorded at RT of (a) the form α of trehalose, (b) the form α after 20 h of annealing at 117 °C, (c) the form α after 50 h of annealing at 117 °C, (d) the form α after 325 h of annealing at 110 °C, and (e) the quenched liquid. The inset shows the X-ray diffraction patterns b−d on an enlarged scale together with the X-ray diffraction pattern of the stable form β of anhydrous trehalose.

For the longest annealing at 117 °C (run 5) and 110 °C (runs 9 and 10), the thermograms show a noticeable deviation of the baseline between 140 and 150 °C. This deviation signals the onset of crystallization toward the stable form β of anhydrous trehalose.[14] For the shorter annealing times, this onset of crystallization occurs at higher temperatures. This difference is due to tiny nuclei of the phase β which will be shown, in the next paragraph, to develop below T_g during very long annealing. Because of these nuclei, the recrystallization is made easier and thus starts at lower temperatures. Melting of phase β then occurs at about 206 °C.

Figure 2 shows X-ray diffraction patterns of trehalose recorded at room temperature after different thermal treatments. Figure 2a corresponds to the phase α of trehalose. The X-ray diffraction pattern of Figure 2b corresponds to the phase α which

has been annealed for 20 h at 117 °C. The Bragg peaks characteristic of the phase α have totally disappeared, and the X-ray diffraction pattern is now made of a large diffusion bump fully similar to that of the quenched liquid (Figure 2e). This X-ray diffraction pattern thus confirms the total amorphization process undergone by the phase α upon annealing below T_g. For longer annealing at the same temperature, the X-ray diffraction pattern of Figure 2c reveals some tiny Bragg peaks which emerge from the diffusion bump. The inset of Figure 2 reveals that these tiny Bragg peaks are not reminiscent of the phase α but clearly correspond to nuclei of the stable phase β of anhydrous trehalose. Since, the nuclei of phase β were not detected by X-ray diffraction before the total disappearance of Bragg peaks characteristic of the phase α, the nuclei of phase β are certainly not present in the sample before the annealing stage. They are thus not formed in parallel with the phase α during the initial dehydration of T_{2H_2O}, as it has been found to occur under some specific dehydration conditions.[16]

The X-ray diffraction pattern of Figure 2d has been recorded after a 325 h annealing at 110 °C. It shows essentially the same features as that recorded after 50 h of annealing at 117 °C (Figure 2c), that is, no more Bragg peaks characteristic of the phase α and tiny Bragg peaks characteristic of the phase β which superimpose onto a broad diffusion bump. However, contrary to the annealing at 117 °C, no "Bragg peak free" X-ray diffraction pattern could be observed for shorter annealing. This indicates that, at this temperature, the nuclei of the phase β start to develop before the phase α has been totally amorphized. Upon heating, the nuclei of phase β promote the recrystallization of the large amorphous fraction of the annealed samples toward this phase. They are thus responsible for the depression of the onset of recrystallization which has clearly been observed in the DSC scans of Figure 1 for the longest annealing times (runs 5, 9, and 10).

4. Discussion

The thermograms of Figure 1 show that annealings of the phase α below T_g and T_m (runs 3−12) result in a decrease of the melting peak upon heating and the concomitant development of a C_p jump signaling the formation of a glass. This indicates that the initially crystalline form α undergoes a slow isothermal vitrification upon annealing below T_g.

This isothermal vitrification process requires that the phase α has a free enthalpy higher than that of the amorphous state. In other words, that means that the phase α turns out to be in a very unusual superheating situation similar to that sketched in Figure 3. The metastability release then occurs through a slow but spontaneous vitrification process below T_g. This behavior implies that the effective melting temperature (T_m^{eff}) of phase α is located below 105 °C (T_m - 18 °C). The possibility to bypass this temperature and to bring the phase α in a metastable situation with respect to the amorphous state is due to the fact that the effective melting temperature is located far below T_g. This makes the phase α thermodynamically unstable but dynamically frozen in the range [T_m^{eff}, T_g]. In this temperature range, the isothermal kinetics of vitrification strongly slows down upon cooling because the molecular mobility decreases as we get deeper in the glassy domain, and also because the driving force to the amorphous state vanishes upon approaching T_m^{eff}. Conversely, upon heating at 5 °C/min, the apparent melting of phase α thus appears just above T_g where the large enough mobility permits the metastability release through a rapid amorphization of the sample.

The reason which makes possible the superheating of the crystalline phase α is thus intrinsically different from those

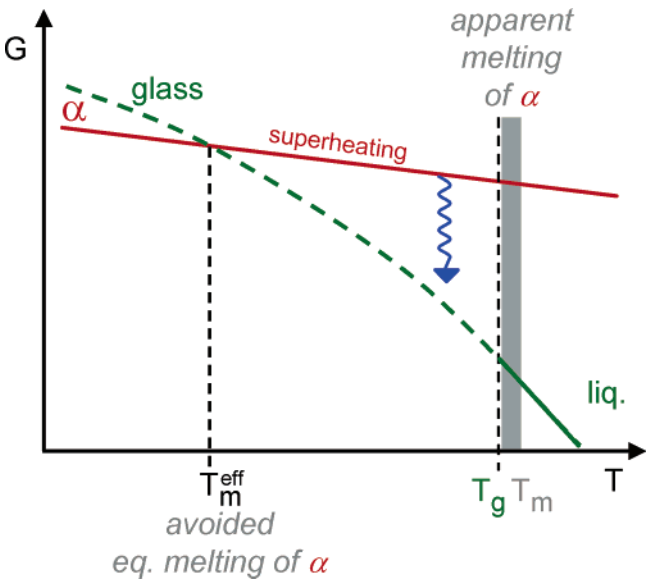

Figure 3. Schematic free enthalpy diagram illustrating the superheating conditions of the phase α between its effective melting temperature (T_m^{eff}) and the glass transition temperature (T_g) above which the melting can no longer be repressed. The undulated arrow represents the slow metastability release of the superheated state by vitrification during an isothermal annealing below T_g.

usually invoked to explain the superheating of metals. For these latter systems, superheating situations are generally reached by ultrafast heating rates[10] and by eliminating as much as possible free surfaces and grain boundaries which both strongly promote the heterogeneous nucleation of the liquid phase.[6−8] For trehalose, the situation is different. The heterogeneous nucleation is not really avoided but strongly slowed because of the low molecular mobility (or high viscosity) of the liquid nuclei appearing below T_g.

In the absence of heterogeneous nucleation, the melting mechanism of a crystalline phase just above T_m is expected to be similar to the crystallization mechanism of an undercooled liquid just below T_m. In both cases, the transformation is expected to occur through a homogeneous nucleation and growth process which usually governs the decay of metastable states. However, because the molecular mobility rapidly increases when heating, the nucleation of the liquid phase upon melting is much more rapid and then much more difficult to study than the nucleation of crystal in the undercooled liquids. From that point of view, the phase α of trehalose offers an exceptional situation to study the homogeneous nucleation regime which is made very slow by the glassy character of the nucleating liquid. This makes it possible to reach and to observe the homogeneous liquid nucleation regime, even if this observation is likely to be spoiled by a parallel heterogeneous nucleation process which, a priori, cannot be avoided. Moreover, for larger superheating, the mean field theories for first-order transitions predict the existence of a spinodal temperature (T_{sp}^{α}) above which the crystalline phase α is expected to become unstable with respect to the liquid phase. If this absolute limit of metastability of the phase α is located far enough below T_g, it should be potentially possible to observe the instability regime by heating rapidly the sample between T_{sp}^{α} and T_g. Investigations of these aspects are actually in progress.

According to Ostwald's rule of stages,[17] the kinetic pathway between the dehydrated T_{2H_2O} and the stable crystalline form β can involve transient states which are energetically less stable than the phase β but kinetically easier to reach. From our

experiments, it appears clearly that this kinetic pathway is the following:

$$\text{dehydrated } T_{2H_2O} \rightarrow \alpha \rightarrow \text{amorphous state} \rightarrow \beta \quad (1)$$

The original aspect of this sequence is that the crystalline phase α precedes the formation of the amorphous state. We may think that this kind of behavior also occurs during the dehydration of a number of crystalline hydrates, but this has not yet been detected because the amorphous state is nearly instantaneously reached if the dehydration is performed above the glass transition temperature, as is generally the case. In future works, it will thus be worth searching for this kind of situation in crystalline hydrates which can be dehydrated below the glass transition temperature of their corresponding liquid state.

5. Conclusion

Our investigations show that the crystalline form α of anhydrous trehalose experiences superheating conditions when heated in the range $[T_m^{eff}, T_g]$ where the effective melting temperature (T_m^{eff}) is at least below 105 °C (T_g − 15 °C). This unusual behavior is made possible by the very low molecular mobility of the liquid phase below T_g which strongly slows down the melting process. The metastability release of the phase α between T_m^{eff} and T_g then occurs through a slow isothermal vitrification process whose kinetics strongly depends on the temperature. The phase α of trehalose thus appears to be a very convenient system to study in detail the physical mechanisms which govern the metastability breaking of crystalline phases toward the liquid phase above their melting point.

Acknowledgment. This work was performed in the framework of an Interreg III network between Nord-Pas de Calais and Kent.

References and Notes

(1) Debenedetti, P. G. *Metastable Liquids—Concepts and Principles*; Princeton University Press: 1996.
(2) Debenedetti, P. G.; Stillinger, F. H. *Nature* **2001**, *410*, 259.
(3) Cahn, R. W. *Nature (London)* **1986**, *323*, 668.
(4) Maddox, J. *Nature (London)* **1987**, *330*, 599.
(5) Dash, J. G. *Rev. Mod. Phys.* **1999**, *71*, 1737.
(6) Daeges, J.; Gleiter, H.; Perepezko, J. H. *Phys. Lett. A* **1986**, *119*, 79.
(7) Lu, K.; Jin, Z. H. *Curr. Opin. Solid State Mater. Sci.* **2001**, *5*, 39.
(8) Shvartsburg, A. A.; Jarrold, M. E. *Phys. Rev. Lett.* **2000**, *85*, 2530.
(9) Kaykin, S. E.; Bene, N. P. *Acad. Sci. USSR* **1939**, *23*, 31.
(10) Herman, J. W.; Elsayed, A. H. E. *Phys. Rev. Lett.* **1992**, *69*, 1228.
(11) Sussich, F.; Urbani, R.; Cesaro, A.; Principalle, F.; Bruckner, S. *Carbohydr. Lett.* **1997**, *2*, 403.
(12) Sussich, F.; Urbani, R.; Princivalle, F.; Cesaro, A. *J. Am. Chem. Soc.* **1998**, *120*, 7893.
(13) Sussich, F.; Cesaro, A. *J. Therm. Anal. Calorim.* **2000**, *62*, 757.
(14) Willart, J. F.; De Gusseme, A.; Hemon, S.; Descamps, M.; Leveiller, F.; Rameau, A. *J. Phys. Chem. B* **2002**, *106*, 3365.
(15) Keller, A.; Hikosaka, M.; Rastagi, S.; Toda, A.; Barham, P. J.; Goldbeck-Wood, G. *J. Mater. Sci.* **1994**, *29*, 2579.
(16) Taylor, L. S.; York, P. *J. Pharm. Sci.* **1998**, *87*, 347.
(17) Ostwald, W. *Z. Phys.* **1897**, *22*, 286.